3424 *Chem. Mater.* **2009,** *21,* 3424–3432
DOI:10.1021/cm901225s

CHEMISTRY OF MATERIALS
Article

Hybrid Materials Combining Photoactive 2,3-DidecyloxyAnthracene Physical Gels and Gold Nanoparticles

Neralagatta M. Sangeetha,[†] Shreedhar Bhat,[†] Guillaume Raffy,[†] Colette Belin,[†] Anne Loppinet-Serani,[‡] Cyril Aymonier,[‡] Pierre Terech,[§] Uday Maitra,[⊥] Jean-Pierre Desvergne,[†] and André Del Guerzo*[,†]

[†]*Université de Bordeaux, CNRS, Institut des Sciences Moléculaires, 351 Cours de la Libération, 33405 Talence Cedex, France,* [‡]*CNRS, Université de Bordeaux, ICMCB, 87 Avenue Albert Schweitzer, 33608 Pessac Cedex, France,* [§]*CEA, INAC-SPrAM-LASSO, 17 rue des Martyrs, 38054 Grenoble, France, and* [⊥]*Department of Organic Chemistry, Indian Institute of Science, 560012 Bangalore, India*

Received May 4, 2009. Revised Manuscript Received June 11, 2009

Organic/inorganic hybrid gels have been developed in order to control the three-dimensional structure of photoactive nanofibers and metallic nanoparticles (NPs). These materials are prepared by simultaneous self-assembly of the 2,3-didecyloxyanthracene (DDOA) gelator and of thiol-capped gold nanoparticles (AuNPs). TEM and fluorescence measurements show that alkane-thiol capped AuNPs are homogeneously dispersed and tightly attached to the thermoreversible fibrillar network formed by the organogelator in *n*-butanol or *n*-decanol. Rheology and thermal stability measurements reveal moreover that the mechanical and thermal stabilities of the DDOA organogels are not significantly altered and that they remain strong, viscoelastic materials. The hybrid materials display a variable absorbance in the visible range because of the AuNPs, whereas the strong luminescence of the DDOA nanofibers is efficiently quenched by micromolar amounts of AuNPs. Besides, we obtained hybrid aerogels using supercritical CO_2. These are very low-density porous materials showing fibrillar networks on which fluorinated gold NPs are dispersed. These hybrid materials are of high interest because of their tunable optical properties and are under investigation for efficient light scattering.

1. Introduction

Hybrid materials are attractive for a large range of applications because of their novel and tunable properties. Among these, one can mention optically active materials that require organization of dispersed nano-objects into structures of controlled optical properties designed for optoelectronics, metamaterials, waveguides, lasers, sensors, or other smart materials. Along theses lines, self-assembly has been explored to induce structuring of hybrid materials of various sorts, including by the use of molecular physical gels and in particular "gels of low molecular mass compounds (M_w < 1000)".[1] The latter are thermoreversible, viscoelastic soft materials, often consisting of complex 3D self-assembled fibrillar networks (SAFINs) that imprison organic solvents (organogels), water (hydrogels) or supercritical fluids (leading to aerogels after fluid removal). When these fibers consist of oligo-phenylene-vinylenes, perylenes, coronenes, or acenes that are highly ordered into rodlike or tape-like anisotropic nano-objects, these assemblies can display anisotropic optical or optoelectronic properties for the aforementioned applications.[2] As an advantage over polymeric gels, the noncovalent interactions such as $\pi-\pi$, hydrogen bonding, donor−acceptor, and hydrophobic interactions between the organogel building blocks can be tuned and tailored according to the desired applications, resulting in a novel class of functional materials.

In recent years, nanostructured hybrid gels have been prepared by either entrapping the colloidal species inside a gel, covalently bonding self-assembled NPs onto a gel network or dissolving the NPs inside the gel network.[3] An attractive approach to control the internal organization of hybrid materials is to use noncovalent, supramolecular interactions. For example, arrangements of metal NPs have been obtained using gel composites,[4] tapes,[5] fibers,[6] and organic small molecular templates.[7]

*Corresponding author. E-mail: a.del-guerzo@ism.u-bordeaux1.fr.

(1) For reviews on molecular gels and aerogels: (a) Molecular Gels: Materials with Self-Assembled Molecular Fibrillar Networks; Terech, P., Weiss, R. G., Eds.; Springer: Dordrecht, The Netherlands, 2006. (b) Sangeetha, N. M.; Maitra, U. *Chem. Soc. Rev.* **2005**, *10*, 821. (c) Dastidar, P. *Chem. Soc. Rev.* **2008**, *12*, 2699. (d) Estroff, L. A.; Hamilton, A. D. *Chem. Rev.* **2004**, *104*, 1201. (e) Terech, P.; Weiss, R. G. *Chem. Rev.* **1997**, *97*, 3133. (f) Pierre, A. C.; Pajonk, G. M. *Chem. Rev.* **2002**, *102*, 4243. (g) Gesser, H. D.; Goswami, P. C. *Chem. Rev.* **1989**, *89*, 765.

(2) (a) Stupp, S. I. *Chem. Rev.* **2005**, *105*, 1023. (b) Ajayahosh, A.; Praveen, V. K. *Acc. Chem. Res.* **2007**, *46*, 644. (c) Cerveau, G.; Corriu, R. J. P.; Framery, E. *Chem. Mater.* **2001**, *13*, 3373.

(3) Hybrid Materials, Synthesis, Characterization and Applications; Kickelbick G., Ed.; Wiley VCH: Weinheim, Germany, 2007.

(4) (a) Love, C. S.; Chechik, V.; Smith, D. K.; Wilson, K.; Ashworth, I.; Brennan, C. *Chem. Commun.* **2005**, *15*, 1971. (b) Zhang, J.; Xu, S.; Kumacheva, E. *Adv. Mater.* **2005**, *17*, 2336. (c) Ray, S.; Das, A. K.; Banerjee, A. *Chem. Commun.* **2006**, *19*, 2816. (d) Vemula, P. K.; John, G. *Chem. Commun.* **2006**, *21*, 2218. (e) Bhattacharya, S.; Srivastava, A.; Pal, A. *Angew. Chem., Int. Ed.* **2006**, *45*, 2934. (f) Bhat, S.; Maitra, U. *Chem. Mater.* **2006**, *18*, 4224.

(5) van Herrikhuyzen, J.; George, S. J.; Vos, M. R. J.; Sommerdijk, N. A. J. M.; Ajayaghosh, A.; Meskers, S. C. J.; Schenning, A. P. H. J. *Angew. Chem., Int. Ed.* **2007**, *46*, 1825.

Published on Web 07/06/2009

Scheme 1. Schematic Representation of a Hybrid Material (cylinder = fibers; spheres = nanoparticles) and Some Tunable Characteristics[a]

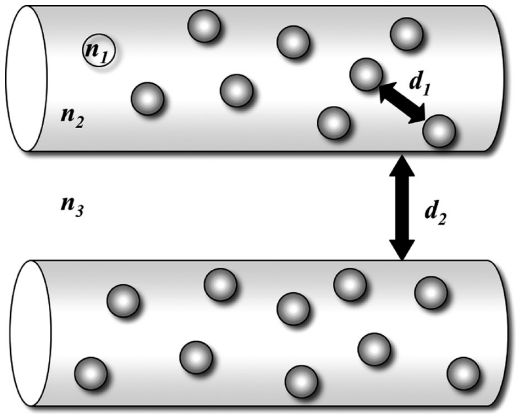

[a] *d* represent the distances between two NPs (d_1) and two fibers (d_2), and *n* the refractive indexes of NPs (n_1), fibers (n_2) and fluid (n_3).

π-extended poly aromatics can absorb and emit light and are studied as semiconducting materials, whereas gold NPs absorb light and influence the luminescence of organic compounds. Moreover, gold NPs and fibers scatter light according to the Mie theory, and thus gold NP dispersions have recently been suggested as candidates for metamaterials with tunable, particle-size-dependent, refractive index.[8] The combination of molecular organogels based on π-extended poly aromatics with inorganic NPs could afford hybrid materials with unprecedented and desired properties. Nevertheless, this way has insufficiently been exploited so far.[5]

Hybrid gels allow the exploration of the concept detailed in scheme 1, in which several parameters of the material could be changed. Indeed, the interfiber distance (d_2 in Scheme 1) and the fiber−fluid interface area could be varied changing the gelator concentration. Similarly, the variation of NP concentration modifies the average distance between NPs (d_1). Further changes reside in the optical properties of the components, such as the absorption, luminescence, birefringence or refractive index (n_2) of the fibers, the environing media (n_3) or the NPs (n_1). We report here our first results on the exploration of gel-nanoparticle hybrid materials based on [*n*]-acenes recognized for their unique photophysical properties and their intriguing gelling properties when substituted with selected pendent chains. Herein are described the synthesis, characterization, and luminescence properties of hybrid materials formed by incorporating thiol-capped gold nanoparticles (AuNPs) into 2,3-didecyloxyanthracene organogels, as well as the preparation of aerogels.

2. Results

2,3-Didecyloxyanthracene (DDOA) is a supergelator in a broad range of organic solvents, yielding soft materials with noticeable thermal and mechanical stabilities.[9] As an alternative to organic solvents, supercritical CO_2 has been used to prepare the low-density DDOA aerogels.[9a] It has been shown that the nature and length of the hydrocarbon chains attached on the anthracene nucleus are of paramount importance for controlling the molecular organization of the gelator, and thus define its gelation ability and the gel's stability. Detailed studies of the gelation and critical gelation concentrations of dialkyloxyacenes have been reported elsewhere,[9] and the molecular structure has been proposed on the basis of a crystallographic study (Chart 1) combined to spectroscopic investigations.[10] The DDOA gels show intense fluorescence, but unexpectedly, no photodimerization could be demonstrated within the gels.[11]

So far, the gelation of solvents by DDOA has shown to occur even in the presence of doping by aromatic compounds (<10%) without drastically altering the fiber network structure. Thus we extrapolated that the organo- and aerogels could serve as a scaffold for the dispersion, stabilization, and organization of inorganic NPs. To favor intercomponent interactions, the NPs were capped with organic ligands and mixed in a suitable medium. A detailed investigation on the hybrid DDOA organo- and aerogels and capped AuNPs are described in the following sections.

2.1. Preparation of Hybrid Organogels and Aerogels. Alkanethiol capped gold nanoparticles (AuNPs, Chart 1) were prepared by the Brust method using a thiol to gold salt molar ratio of 1 so as to yield ~3 nm gold core diameter NPs ($M_w \approx 2 \times 10^5$, see Experimental Section).[12] Thiol/Au ratios of 2 and 4 gave the same results. They display an absorption in the UV range and the expected broad surface plasmon band around 500 nm (shoulder).[12]

Organogels. DDOA forms thermoreversible organogels by cooling a hot alkane or alcohol solution to room temperature in the presence of dispersed alkane capped NPs at a gelator concentration as low as 7.1 mM (0.35% w/v) in *n*-butanol and 12.8 mM (0.63% w/v) in *n*-decanol, and AuNP concentrations below 50 μM (10 mg/mL). The hybrid gels (Figure 1) obtained within minutes do not show any apparent phase separation and are wine red-

(6) Kimura, M.; Kobayashi, S.; Kuroda, T.; Hanabusa, K.; Shirai, H. *Adv. Mater.* **2004**, *16*, 335.
(7) (a) Li, Z.; Chung, S.-W.; Nam, J .-M.; Ginger, D. S.; Mirkin, C. A. *Angew. Chem., Int. Ed.* **2003**, *42*, 2306. (b) Li, L.; Stupp, S. I. *Angew. Chem., Int. Ed.* **2005**, *44*, 1833. (c) Braun, G.; Inagaki, K.; Estabrook, R. A.; Kang, D. Y.; Erickson, K. J.; Taton, T. A. *J. Am. Chem. Soc.* **2005**, *127*, 13800. (d) Koyfman, A. Y.; Braun, G.; Magonov, S.; Chworos, A.; Reich, N. O.; Jaeger, L. *J. Am. Chem. Soc.* **2005**, *127*, 11886. (e) Wood, K.; Levy, E.; Cleland, A. N.; Strouse, G. F.; Reich, N. O. *Langmuir* **2005**, *21*, 10699. (f) Vos, M. R. J.; Etxebarria Jardo, G.; Llanes Pallas, A.; Breurken, M.; van Asselen, O. L. J.; Bomans, P. H. H.; Leclère, P. E. L. G.; Frederik, P. M.; Nolte, R. J. M.; Sommerdijk, N. A. J. M. *J. Am. Chem. Soc.* **2005**, *127*, 16768.
(8) Kubo, S.; Diaz, A.; Tang, Y.; Mayer, T. S.; Khoo, I. C.; Mallouk, T. E. *Nano Lett.* **2007**, *7*, 3418.
(9) (a) Placin, F.; Desvergne, J.-P.; Cansell, F. *J. Mater. Chem.* **2000**, *10*, 2147. (b) Brotin, T.; Utermölhen, R.; Fages, F.; Bouas-Laurent, H.; Desvergne, J.-P. *Chem. Commun.* **1991**, *6*, 416. (c) Desvergne, J.-P.; Olive, A. G. L.; Sangeetha, N. M.; Reichwagen, J.; Hopf, H.; Del Guerzo, A. *Pure Appl. Chem.* **2006**, *78*, 2333.
(10) Olive, A. G. L.; Raffy, G.; Allouchi, H.; Léger, J.-M.; Del Guerzo, A.; Desvergne, J.-P. *Langmuir* **2009**, DOI: 10.1021/la804206n.
(11) Desvergne, J.-P.; Brotin, T.; Meerschaut, D.; Clavier, G.; Placin, F.; Pozzo, J.-L.; Bouas-Laurent, H. *New. J. Chem.* **2004**, *28*, 234.
(12) Hostetler, M. J.; Wingate, J. E.; Zhong, C.-J.; Harris, J. E.; Vachet, R. W.; Clark, M. R.; Londono, J. D.; Green, S. J.; Stokes, J. J.; Wignall, G. D.; Glish, G. L.; Porter, M. D.; Evans, N. D.; Murray, R. W. *Langmuir* **1998**, *14*, 17.

Chart 1. : (A) Structure of the Gelator DDOA and Au Nanoparticles Used. (B) Crystal Structures of the Previously Reported[10] Heptyl Analogue

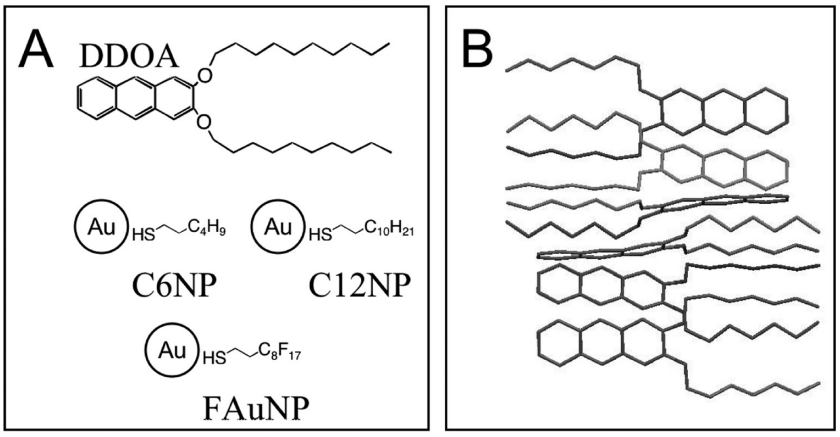

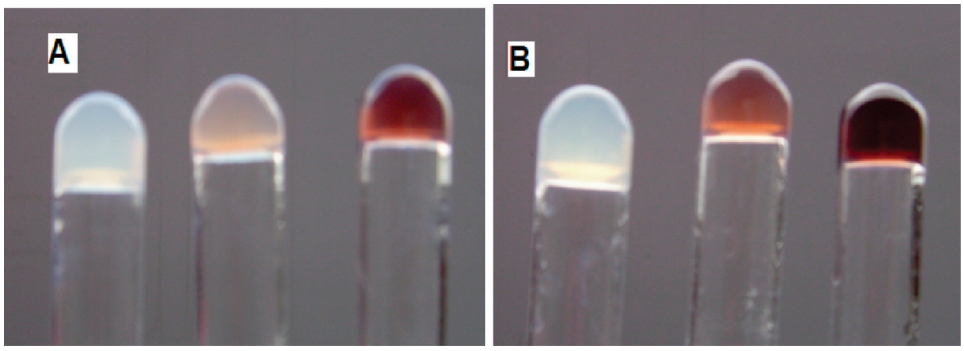

Figure 1. Photographs of (A) *n*-butanol gels of 7.1 mM DDOA (left to right: no AuNP, 0.27 μM, and 1.38 μM C6NP); (B) *n*-decanol gels of 12.8 mM DDOA (left to right: no AuNP, 0.28 μM, and 1.43 μM of C12NP).

colored in the hot solution, whereas the absence of blue-purple tint due to red-shifted absorption indicates that particles are dispersed and stabilized in the SAFIN rather than aggregated.[13] This contrasts with dispersions of *n*-hexanethiol capped AuNPs (C6NP) in *n*-butanol in the absence of gelator, which are wine red only upon heating while they slowly decolorize upon standing at room temperature because of the precipitation of the particles. In *n*-decanol, no dispersion of C6NP could be observed and thus *n*-dodecanethiol capped AuNPs (C12NP) were prepared. Figure 1 shows the photographs of the DDOA gels with increasing quantities of hexanethiol capped NPs in *n*-butanol and dodecanethiol capped NPs in *n*-decanol. The visual appearance of the sealed vials did not change over several months. A similar trend was observed in hydrocarbon solvents like decane and dodecane, in which dodecanethiol capped NP dispersions are more stable in the absence of gelator, but in which DDOA forms more opaque gels only at larger gelator concentrations ($\geq$1% w/v, i.e., 20 mM). In dodecane, DDOA formed gels in a 6.1−61 mM range, with a doping by C12NPs reaching 40 μM for the 61 mM gel.

Aerogels. To drastically change the fluid surrounding the nanofibers, highly porous solvent-free aerogels of DDOA are formed in supercritical CO_2 ($scCO_2$) and obtained after release of CO_2, yielding highly open and luminescent fibrillar networks (Figures 2 and 3).[9a] Supercritical CO_2 is not only promoted as a sustainable solvent in chemical processing but is also essential to obtain these materials. Indeed, the surface tension vanishes in the supercritical phase inducing the absence of liquid−air transition upon solvent removal.[14] Thus, due to decrease of interfacial forces a structured network of DDOA is obtained, whereas a collapsed system would have resulted from organic solvent evaporation (xerogels). To produce such hybrid aerogel material, we attempted to disperse or dissolve both AuNPs and DDOA in supercritical CO_2. This technique was not successful when DDOA was mixed with C6NP or C12NP because the NPs could not be dissolved in $scCO_2$, and thus the aerogels isolated were bare (as seen by TEM).

To overcome this drawback, we prepared gold NPs by the Brust method using a perfluorinated ligand, 1,1,2,2-H-perfluorodecanethiol, as a capping agent. The NPs obtained by this method (see Figure S2 in the Supporting Information) were insoluble in alkanes or toluene, but soluble in trifluorotoluene and displayed also a ~3 nm

(13) Unfortunately, the absorption spectra of hybrid gels are affected by the saturating absorbance in the UV region of DDOA and by high light diffusion in the visible range. A broadband around 520 nm is attributed to the AuNPs (see Figure S1 in the Supporting Information).

(14) Cansell, F.; Aymonier, C.; Loppinet-Serani, A. *Curr. Opin. Solid State Mater. Sci.* **2003**, *7*, 331.

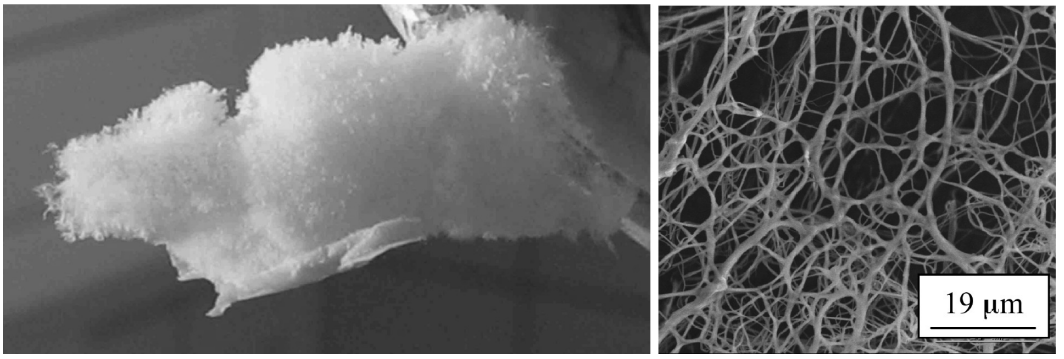

Figure 2. (Left) Photo of an aerogel (about 5 cm long) of DDOA containing FAuNP (see TEM in Figure 6). (Right) SEM microscopy image of a bare DDOA aerogel.

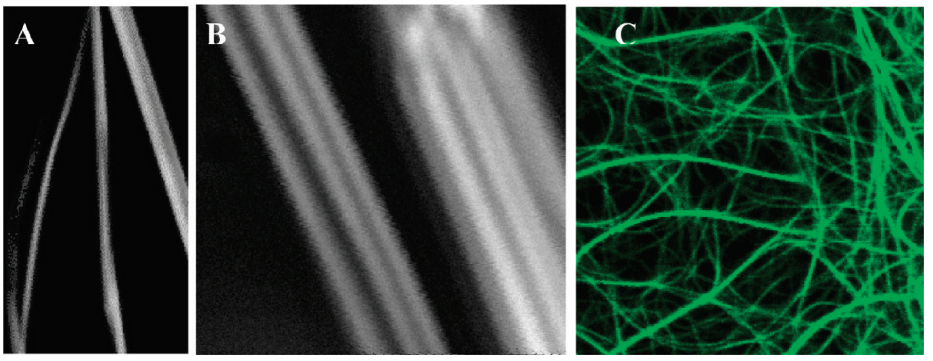

Figure 3. Confocal microscopy images under 385 nm laser excitation of gel samples deposited on a glass slide: (A) fluorescence intensity of a DDOA aerogel ($5 \times 10\,\mu$m, $400 < \lambda_{em} < 450$ nm); (B) backscattering intensity at 385 nm of a hybrid FAuNP-DDOA aerogel ($3.5 \times 4\,\mu$m); (C) fluorescence intensity of a DDOA/butanol organogel (7.1 mM DDOA, $20 \times 20\,\mu$m, $400 < \lambda_{em} < 450$ nm). The organogel is formed directly on the slide and only partial (~25%) solvent evaporation occurred.

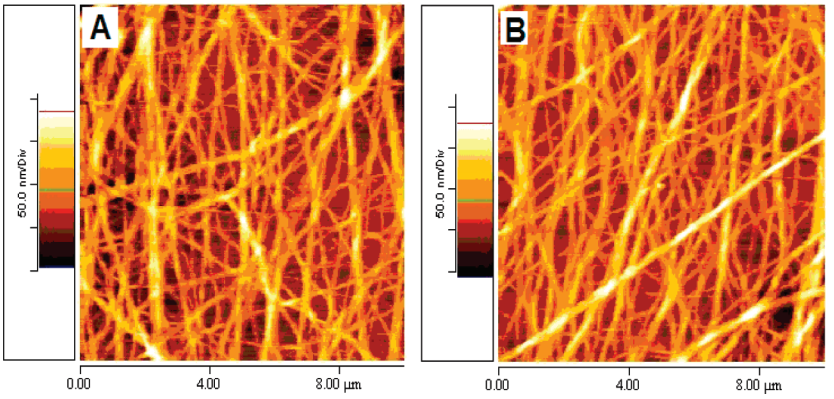

Figure 4. AFM images of the DDOA/*n*-butanol gels (A) without (7.7 mM) and (B) with (8.7 mM) hexanethiol-capped gold NPs (1.88 μM).

core diameter and a surface plasmon band centered at 508 nm. These "FAuNPs" could also be dispersed in $scCO_2$, and DDOA (2 mM) successfully formed aerogels in the presence of the FAuNPs (initially 2 wt % relative to DDOA). In this case, the NPs were successfully embedded in the aerogels (see Figures 5 and 6), although the exact loading could not be determined because some of the material did not disperse.

2.2. Structural Characterization. The structural characterization of hybrid organogels and aerogels was carried out using transmission electron microscopy (TEM) and atomic force microscopy (AFM). The AFM images of the xerogels (dried organogel, Figure 4) of DDOA with and without NPs prepared by spin-coating a small volume of the hot sol on mica showed no morphological differences between the two gels. The AFM images revealed the presence of highly entangled fibrillar networks with fiber diameter ranging between 100 and 200 nm and are infinitely long, sometimes forming bundles. Such values are comparable with those obtained from the noninvasive small-angle neutron scattering technique of the swollen gels, and thinner fibers (10 nm) can also be present.[15] The

(15) (a) Terech, P.; Clavier, G.; Bouas-Laurent, H.; Desvergne, J.-P.; Demé, B.; Pozzo, J.-L. *J. Colloid Interface Sci.* **2006**, *302*, 633. Terech, P.; Desvergne, J.-P.; Bouas-Laurent, H. *J. Colloid Interface Sci.* **1995**, *174*, 258.

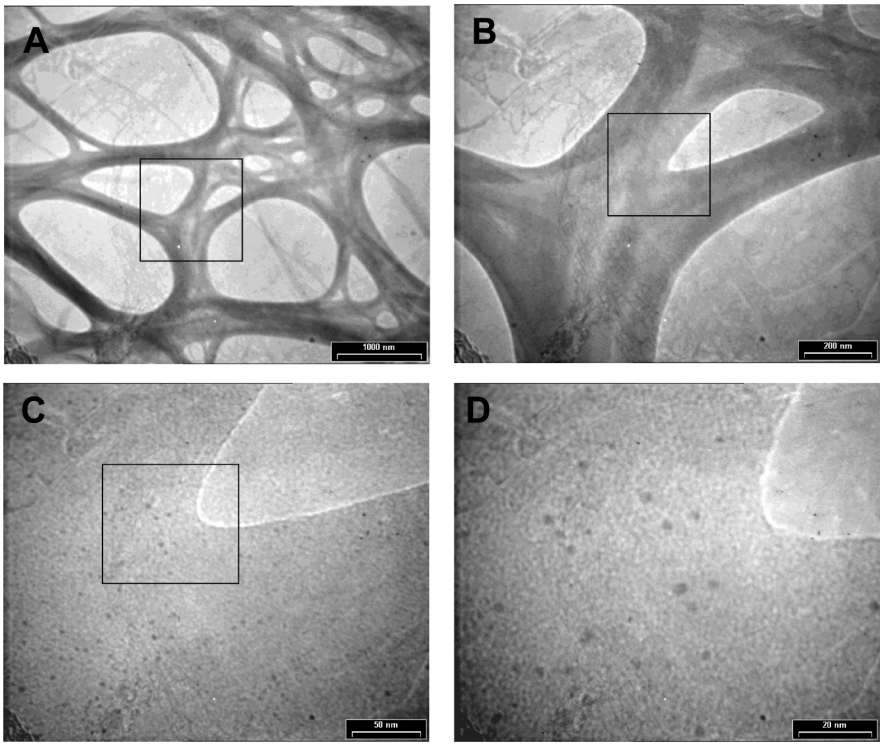

Figure 5. TEM images of a xerogel derived from DDOA/*n*-butanol gel (8.2 mM) with hexanethiol capped gold nanoparticles (0.5 μM) at different magnifications. Scale bars: A, 1000 nm; B, 200 nm; C, 50 nm; D, 20 nm.

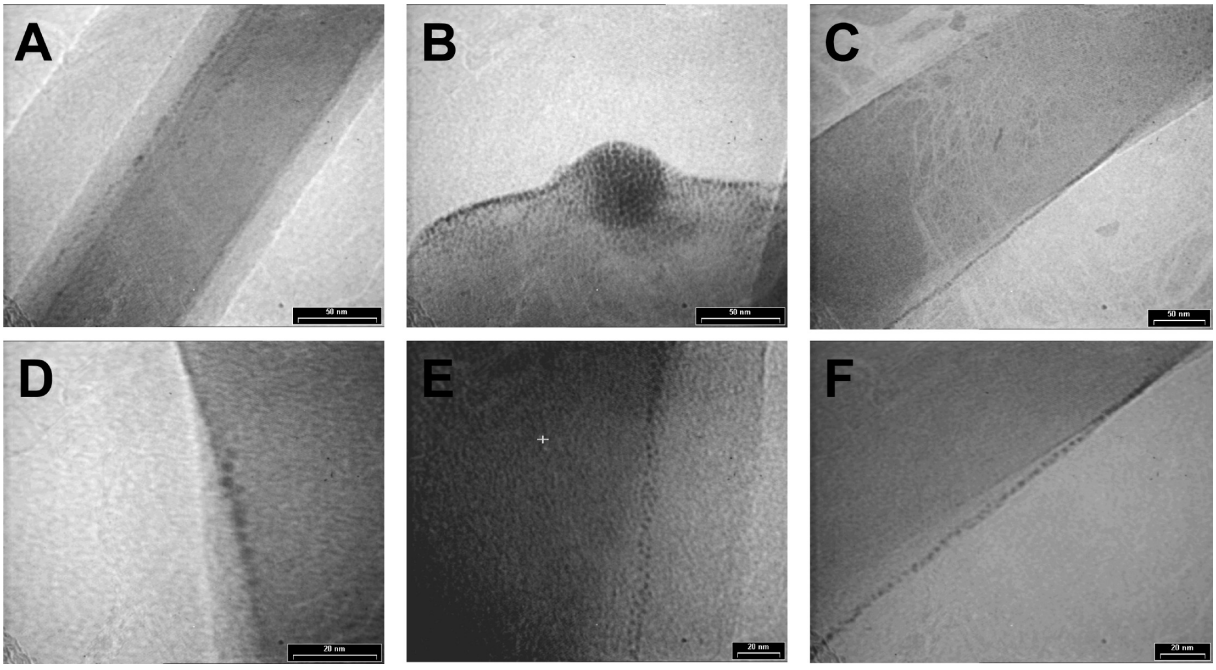

Figure 6. TEM images of aerogels of DDOA prepared in the presence of fluorous gold nanoparticles (FAuNPs). Scale bars: A−C, 50 nm; D−F, 20 nm.

images clearly indicate that the SAFIN was preserved after the AuNP immobilization and that no aggregation of fibers in much thicker bundles was induced. No NP could be detected on the AFM images of the AuNP-gel composites (Figure 4B) as their size is too small to be discerned with the ~6 nm AFM tip. However, the NPs are easily visualized in the TEM of the gels dried on copper grids.

The TEM images of the gel of DDOA/C6NP in *n*-butanol are shown in Figure 5. DDOA forms a SAFIN with bundles of 100−200 nm and NPs distributed uniformly over the fibers. The NPs seem to be all embedded into or onto the fibers as none could be observed in the region outside the fibers. No large aggregates of NPs were observed in the hybrid gel, whereas this was typical when NPs were directly dispersed on the copper grid. The

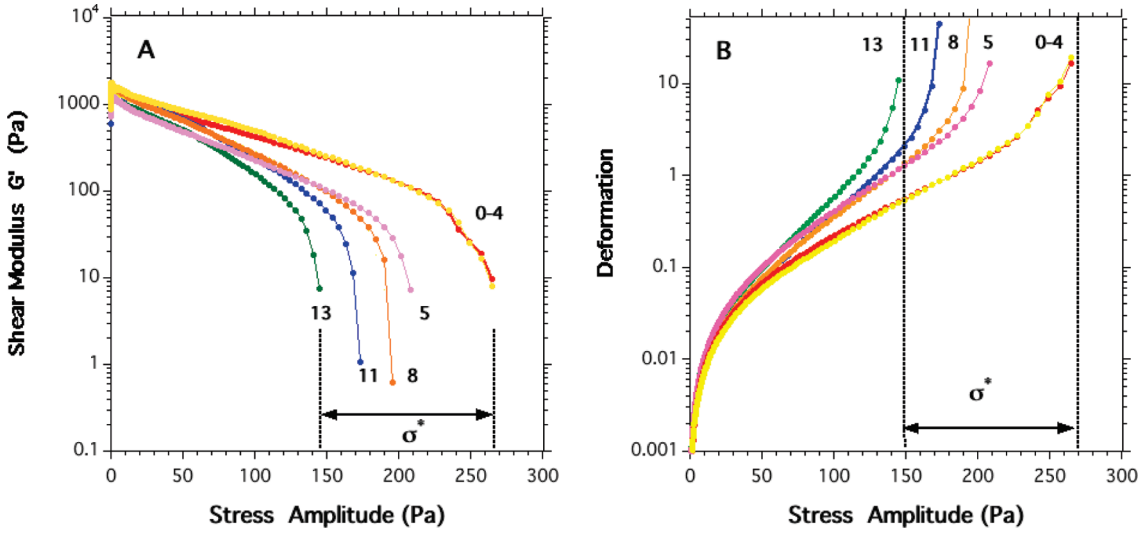

Figure 7. Rheology of DDOA and C12NP/DDOA gels in *n*-dodecane. $C_{DDOA} = 6.1 \times 10^{-2}$ M and labels indicate the AuNP loads ([C12NP]: 0, 4, 5, 8, 11, 13 μM). The range of yield stress (σ*) variations is indicated by arrows. (A) G′ versus applied stress. (B) Deformation versus applied stress.

distance between the NPs in Figure 5D is ca. 5−20 nm with 21 particles in 120 nm^2 of fiber surface (~0.2 NPs/nm^2) for a load in NPs of 6×10^{-3} %mol (NP/gelator % molar ratio).

Slight differences were observed for the aerogels. TEM (Figure 6) shows the presence of NPs on the aerogel fibers and reveals that the distribution of the NPs in the aerogel sample is less uniform as for the organogels. Interestingly, the particles spread as a thin monolayer on the fibers, occasionally in patches, and particularly concentrated on the edges and on the rare ends of the aerogel fibers. It is also interesting to notice that in some cases NPs are nicely aligned individually along a ridge.

2.3. Thermal Reversion of the Physical Organogel. The gel-to-sol transition temperatures (T_{gs}) of the gels depend on the solvent and DDOA concentration and were determined by the inverted test tube method, where sealed tubes containing the hybrid gels are kept upside down in a heating thermostatic water bath (rate +1 K/min) until the gel falls under gravity.[16] T_{gs} values are independent of the presence or not of AuNPs in the ranges studied and are 42, 38, and 47 °C, respectively, for the *n*-dodecane (20.4 mM DDOA; 0−0.5 μM, i.e., 0−0.1 mg/mL C12NP), *n*-decanol (12.8 mM; 0−1.43 μM C12NP), and *n*-butanol gels (7.1 mM; 0−1.38 μM C6NP). The hybrid gels are thus as strong as the free gels, as supported by their rheological behavior.

2.4. Rheological Properties. Rheological measurements of DDOA gels in dodecane (6.1 mM, 3% w/v) show that they exhibit high shear storage moduli, typically $G' \approx 1700 \pm 200$ Pa and high yield stress values, typically $\sigma^* \approx 270$ Pa. Such flow characteristics are qualitatively similar to those observed for a hydroxystearate organogel reference system.[17] Both systems have SAFINs presenting nodal zones where fibers are merging in crystalline microdomains. Previous X-ray scattering experiments of DDOA gels and homologues[15] have shown that their nodal zones were bundles of fibers presenting hexagonal arrangements related to those found in the solid phase.

The presence of C12NPs (0−13 mM) in DDOA/dodecane gels (6.1 mM) does not significantly alter the shear storage modulus G' at zero-shear ($1750 < G' < 1250$ Pa), as shown in Figure 7A. In this range, the volume fraction of added NPs remains weak compared to that of the elastically active 1D species in the DDOA gel networks and, as expected, the shear modulus remains roughly constant. The failure of the NP-decorated gel networks occurs at σ* and the corresponding values slightly decrease from 270 to 150 Pa with the addition of NPs as shown in the log-lin plot of Figure 7A. To explain this increased fragility we propose that the beadlike NPs inserted within the bundles of the hybrid gels decrease the number of contacts per unit length of fibers in the bundles and thereby lead to a decrease of the yield stress. Such a mechanism, acting as a ball bearing, amplifies the slippages between the fibers in a gel undergoing the increasing applied stress. These effects are further revealed in a plot of the deformation versus the stress amplitude (Figure 7B). The strain of the NP-DDOA hybrid SAFINs exhibit strong nonlinear effects, and a dependence upon the NP content is observed. In particular, in the region preceding the divergent strain at σ*, enhanced slopes of the deformation profiles are observed with increasing NP content. Additional X-ray scattering experiments are in progress to explore the structural implications of the NP insertion in the DDOA networks and their consequences on the yielding mechanisms.

2.5. Fluorescence Properties. The investigation of the fluorescence properties of the hybrid gel covers two purposes. First, the DDOA nanofibers emit light (Figure 3C) with high quantum yields and low energy loss,[18] with an

(16) Terech, P.; Rossat, C.; Volino, F. *J. Colloid Interface Sci.* **2000**, *227*, 363.
(17) Terech, P.; Rodriguez, V.; Barnes, J. D.; McKenna, G. B. *Langmuir* **1994**, *10*, 3406.
(18) Del Guerzo, A.; Olive, A. G. L.; Reichwagen, J.; Hopf, H.; Desvergne, J.-P. *J. Am. Chem. Soc.* **2005**, *127*, 17984.

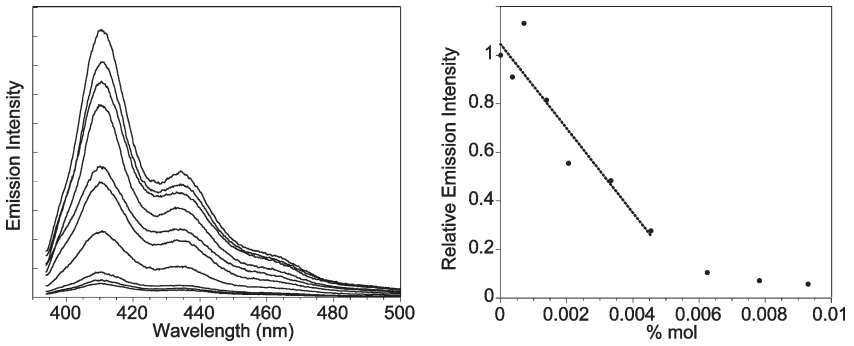

Figure 8. Fluorescence spectra of hybrid gels in butanol with the addition of hexanethiol capped gold nanoparticles (DDOA: 6.5 mM, C6NP: 0−0.62 μM, λ_{ex} = 384 nm): (left) Emission spectra; (right) Relative emission intensity at λ_{em} = 410 nm vs molar percentage of C6NP compared to DDOA. The straight line is a linear regression of the first 7 points.

intensity that is expected to be modulated by the NPs. Second, the fluorescence intensity variation can afford an indirect and macroscopic probing of the homogeneity of the dispersion of NPs in the SAFIN without using a drying process. Figure 8 shows the emission spectra of a DDOA/*n*-butanol gel displaying structured emission bands typical of the self-assembled DDOA molecules.[11,18] With the addition of very small concentrations of gold NPs (< 1μM), the fluorescence intensity of the DDOA organogel strongly decreases without any change of the spectrum. Quenching of organic dye emission by AuNPs has been extensively observed[19] and is generally due to energy or electron transfer, or the enhancement of nonradiative deactivation pathways. These mechanisms can be at the origin of the quenching of DDOA, because we have confirmed that the decrease in emission does not result from excitation light absorption by the NPs, which absorb weakly even for the largest concentrations used in the titration.

Figure 8 represents the relative peak emission intensity as a function of molar percentage of added AuNPs. It confirms that the quenching efficiency is quite spectacular and reaches 50% with only 0.2 μM of C6NPs in a 6.5 mM DDOA/*n*-butanol gel (3×10^{-3} %mol, i.e. 3×10^{-5} molar ratio). At low concentrations, the variation of quenching is almost linearly related to the doping, in agreement with a homogeneous dispersion of the NPs. 90% quenching of the fluorescence occurs at 6×10^{-3} % mol doping in conditions at which TEM measurements (Figure 5) also show a good dispersion of the NPs and a local surface coverage of ~0.2 NPs/nm^2 (i.e., ~5 nm^2/NP). In DDOA/*n*-decanol gels, fluorescence measurements are less precise because of the higher absorbance of the material, but the results are similar. These outstanding quenching efficiencies, occurring for micromolar concentrations, cannot be assigned to a pure diffusion process and can be explained only by tight interactions of the NPs with the fluorescent SAFIN. In the gel, one NP can quench the emission of thousands of DDOA's (according to the linear regression in Figure 8, an average estimate is 1.6×10^4 molecules). This is in agreement with the previous characterization of efficient quenching of ~1×10^3 DDOA's by one tetracene derivative directly incorporated in the gel fibers.[18] Donor-to-donor exciton hopping along the fibers highly increases the total quenching efficiency by the energy acceptor, such as confirmed by studies in DDOA[20] and in organogels of other π-conjuguated compounds.[21] These mechanisms should thus also intervene in the present case and preclude any other photoreactions, such as dimerizations.

3. Discussion

The combination of TEM imaging and fluorescence measurements clearly shows that gold NPs can be dispersed efficiently in organogels and fairly in aerogels by interaction of the particles with the SAFIN. Rheology, TEM and AFM data show that the dispersion occurs without significantly disrupting or modifying the fibrillar network. In organogels, the driving force for the hybrid material formation is mainly due to, besides the self-assembly of the gelators, the weak supramolecular interaction between the alkane chains of the capped NP and those of the DDOA. In addition, the partial solvophobicity at RT of the NPs may contribute to drive them onto the gel network. TEM images to not allow do determine whether the NPs are interacting only on the surface of the fibers, or are completely embedded inside the fibers. Nevertheless, the data on the aerogels suggest that, at least in that case, interaction occurs essentially on the edges of the fibers, and that NPs are not inside the aerogel fibers. In organogels, a direct conclusion cannot be drawn but trapping of NPs in-between fibers forming bundles can be envisaged in the light of the exceptionally high fluorescence quenching efficiency and the slight decrease in yield stress. This study also shows that a tuning of the alkane chain length and its nature is necessary to favor the NP's dispersion in the solvent at high temperatures before the formation of the SAFIN. Thus, although short hexanethiol capping of the NPs is used in butanol, long dodecanethiol capping is required in decanol and perfluorinated thiol capping is essential in $scCO_2$. Interestingly, even if the AuNPs are insoluble at RT, a good

(19) (a) Dubertret, B.; Calame, M.; Libchaber, A. J. *Nat. Biotechnol.* **2001**, *19*, 365. (b) Huang, T.; Murray, R. W. *Langmuir* **2002**, *18*, 7077. (c) Fan, C.; Wang, S.; Hong, J. W.; Bazan, G. C.; Plaxco, K. W.; Heeger, A. J. *Appl. Phys. Sci.* **2003**, *100*, 6297.

(20) Olive, A. G. L. et al.. To be published.

(21) Ajayaghosh, A.; Praveen, V. K.; Vijayakumar, C.; George, S. J. *Angew. Chem., Int. Ed.* **2007**, *46*, 6260.

dispersion is obtained in the organogel. In DDOA organogels, no significant influence of the length of the alkanethiols is observed and the NP−fiber interaction is clearly preferred over self-aggregation. In contrast, in aerogels, the fluorinated NPs display a higher tendency to self-associate indicating that particle−particle interaction is competitive with particle−fiber interaction. It is nevertheless noticeable that "single layer" particle-fiber interaction is favored over multilayer particle−particle aggregation and that thus particle−fiber interaction plays a role at the fiber−air interface.

The good dispersion of AuNPs at the surface of the fibers has a strong impact on the optical properties of the material. Besides an even color change in the visible range due to the absorption by the AuNPs, the strong fluorescence of the DDOA fibers is efficiently and homogeneously quenched by the particles. Additionally, a modulation of the light-scattering properties of this hybrid material is expected, as preliminary microscopy studies have shown that the fibers backscatter light (see Figure 3B), although we have not yet fully characterized this process. These self-assembled fibers offer a scaffold to modulate the dispersion of AuNP, as well as a tuning of the optical properties of the scaffold itself (absorption, fluorescence, light scattering, refractive index). Indeed, the linear decrease of fluorescence intensity with increasing load of NPs ($< 0.5\ \mu$M) indicates not only a homogeneous dispersion of the NPs, but suggests a regular decrease of the average interparticle distance (d_1, see Scheme 1). The interfiber distance (d_2) extends from none to hundreds of nanometers and its average value should in principle depend on the gelator's concentration. Furthermore, the results show that the choice of NP capping can influence whether a homogeneous dispersion or an alignment of NPs along the edges of the fibers occurs. We have also shown that the refractive index of the material can be changed, because n_3 of the fluid varies from $1.40 < n_3 < 1.44$ in organogels (alcohols or alkanes) to $n_3 = 1.00$ in the aerogel (air), whereas for the fibers, n_2 is estimated to be $\sim$1.5. The variation of the optical properties of the AuNPs, such as the absorption spectrum or the refractive index (n_1), is expected to be easily implemented by slightly changing their size.[8] Supplementary perspectives open up for these hybrid materials when one considers previous work. Indeed, macroscopic alignment of the DDOA fibers in organogels can be achieved,[22] and a larger variety of gels are accessible by changing the gelator. In the *n*-acene family, we have developed tetracene and pentacene gelators[23] that can be used in other solvents and present more red-shifted absorption spectra as well as a potential as semiconductors. Future developments also include the synthesis of novel aerogelators.

(22) Shklyarevskiy, I. O.; Jonkheijm, P.; Christianen, P. C. M.; Schenning, A. P. H. J.; Meijer, E. W.; Del Guerzo, A.; Desvergne, J.-P.; Maan, J. C. *Langmuir* **2005**, *21*, 2108.

(23) (a) Reichwagen, J.; Hopf, H.; Del Guerzo, A.; Belin, C.; Desvergne, J.-P.; Bouas-Laurent, H. *Org. Lett.* **2005**, *7*, 971. (b) Desvergne, J.-P.; Del Guerzo, A.; Bouas-Laurent, H.; Belin, C.; Reichwagen, J.; Hopf, H. *Pure Appl. Chem.* **2006**, *78*, 707. (c) Reichwagen, J.; Hopf, H.; Desvergne, J.-P.; Del Guerzo, A.; Bouas-Laurent, H. *Synthesis* **2005**, *20*, 3505.

4. Conclusion

We have demonstrated that an accurate combination of alkane chain derivatized gelator, alkane-capped gold NPs, and alkanes or long chain alcohols leads to the formation of physical composite organogels. The hybrid material formation is driven mainly by the supramolecular interaction of the ligands on the NP and the gelator. In the presence of solvent, the network can be undone easily by heating and the NPs released, whereas the dispersion is stable in the gel at RT. The NPs do not significantly affect the thermal, structural, and mechanical properties of the gel, but modify the absorption and luminescence properties of the material. In perspective, further optical properties such as scattering and refraction of the hybrid material could be modulated by the choice of gelator, NPs and their capping, as well as the solvent. Currently, we are developing tools to characterize appropriately the scattering properties and investigations are also currently being performed with hybrid materials including metal-oxide NPs.

5. Experimental Section

5.1. Materials and Methods. *a. General.* All solvents used were double distilled prior to use or of ACS grade. Gold chloride, $NaBH_4$, 1H, 1H, 2H, 2H-perfluorodecane thiol, 1-hexane thiol, and 1-dodecane thiol were purchased from Aldrich and used as received. All the glassware was acid-rinsed prior to detergent wash and dried after acetone wash. A Hitachi F-4500 spectrofluorimeter and Cary 5000 were used for UV−visible and luminescence measurements in a quartz cell with path length of 1 cm.

b. Synthesis of Gold Nanoparticles (AuNPs). The gold NPs used for the study, dodecanethiol-capped (C12NP) and hexanethiol-capped (C6NP) NPs, were prepared by the classical Brust's two-phase methodology.[12] In a typical procedure, $HAuCl_4$ was extracted into toluene using the phase transfer catalyst tetrahexylammonium iodide. The orange toluene phase was then stirred with appropriate thiol (with S/Au ratio of 1, 2, and 4) for about 15 min, when the color turned pale yellow. To this solution was added $NaBH_4$ in water over a period of 30 s under vigorous stirring. Immediately upon addition, the solution turned colorless first and then wine red. This solution was stirred further for a period of 3−4 h. The brown colored organic layer is separated from that of water and the solvent removed in vacuo to obtain a dark solid. This solid was then sonicated with EtOH and the suspended black solid collected by filtration and washed with copious amounts of ethanol and acetone. The solid was collected and air-dried. According to literature,[12] a 3 nm diameter AuNP (bare 2.73×10^{-19} g/NP) is capped with $\sim$190 thiols, thus yielding 3.3×10^{-19} g/NP $= 2 \times 10^5$ g/mol for C6NP and C12NP.

c. Preparation of Fluorous Thiol-Capped AuNPs (FAuNPs). $HAuCl_4$ (25 mg, 0.063 mmol) was stirred with a solution of tetrahexylammonium iodide (80 mg, 0.166 mmol) in toluene (15 mL). The orange colored toluene layer was separated and stirred with 0.015 mL of 1H, 1H, 2H, 2H-perfluorodecane thiol for 15 min. To this solution was added a solution of $NaBH_4$

(25 mg, 0.66 mmol) in water (1.5 mL) within a period of 30 s with vigorous stirring. The orange solution first clears up and then turns to wine red. As the stirring was continued, froth developed in the reaction mixture. This mixture was stirred overnight. A black solid had separated out which was found sticking to the aqueous layer of the reaction mixture. The organic layer was removed by decantation and ethanol was added to the NP water mixture to obtain a dark red dispersion of the NPs. This dispersion was filtered to remove black solid particles and the solvent removed in vacuo to obtain a dark solid that was washed several times with toluene and $CHCl_3$ (by sonicating the solid with the solvent followed by decantation). The solid so obtained after purification could not be dispersed in common organic solvents like toluene, chloroform, ethylacetate, acetone, tetrahydrofurane, hexanes, etc. However, it can be readily dispersed in fluorous solvents like trifluorotoluene.

d. Synthesis of Wet Hybrid Gels. The wet gel−NP composite was prepared by a simple heating of a mixture of the gelator and the alkane thiol stabilized gold NPs of ~3 nm diameter. Typically, gelator (0.2−3.0% w/v) and powdered NPs in required solvent (1 mL) was heated until the solid was completely dissolved and slowly cooled to room temperature. The gel formation was detected within the first 10 min of cooling.

e. Synthesis of Hybrid Aerogels. The gel formation in supercritical CO_2 (carbon dioxide) was done by following our earlier reports. Typically, 12−20 mg of DDOA in the form of a powder and the capped AuNPs (solid or a suspension or a solution) were charged into a 25 mL steel reactor with a Teflon or aluminum lining and the system was heated to 80 °C. A pressure of 250 bar was then applied and the temperature stabilized between 90 and 95 °C. Under these conditions, DDOA and the AuNPs were allowed to dissolve in supercritical CO_2 for about an hour. After 1 h, the system is cooled to 40 °C and the pressure dropped to 100 bar. Now, the pressure is released in such a way that the conditions do not cross liquid−vapor CO_2 curve. The material isolated from the top portion of the reactor was a white, light fibrous solid or aerogel (yield ~8−10 mg).

f. TEM Imaging. A carbon-coated copper grid was allowed to contact the ready-made wet gel so that a thin film of the gel is formed on the grid. The samples were dried in air for few seconds and then in a vacuum desiccator prior to imaging. Similarly, aerogels were allowed to touch the copper grid carefully to keep a thin layer on the grid and imaged without special desiccation.

5.2. Microscopy and Rheology. *a. AFM Imaging*. The samples were prepared by spin coating ~0.1 mL of the hot sol (both hybrid and bare gels) on a freshly cleaved mica sheet (area ~ 1 × 1 cm). After vacuum drying, the dry gel film was imaged using tips of ~6 nm end diameter on a Thermomicroscope CP AFM. Measurements were done in tapping mode.

b. Confocal Microscopy. Fluorescence images have been obtained with a Picoquant Microtime 200 microscope, using the Symphotime software, coupled to a pulsed picosecond laser (6 ps pulses) operating at about 4.8 MHz frequency, tuned at 770 nm and frequency doubled in a SHG unit generating 385 nm pulses. For images A and C in Figure 3, the fluorescence was filtered with an interference band-pass filter at 425 ± 25 nm. For Figure 3B, images were obtained with the same setup without using band-pass filters. The contribution of the fluorescence in Figure 3B has been measured and is negligible. The aerogel samples were placed on a glass cover slide with tweezers. The organogel was formed directly on the cover slide by drop-casting a hot solution of DDOA in butanol. Measurements have been performed within a few minutes in order to minimize solvent evaporation.

c. Rheology. The rheological properties of wet hybrid gels were measured on a stress-controlled RheoStress 600 (Thermo-Haake) rheometer. A serrated plate−plate geometry (d = 35 mm) was used in all measurements. The temperature of the plates was controlled at 20 °C with an error of ± 0.1 °C. All gels were prepared and stabilized at least 12 h before the measurements. A piece of gel (~1 mL) was scooped and placed on the serrated plate for every individual experiment. The solvent evaporation was kept minimized by using a glass cover on the stator. The device keeps confined a saturated gaseous solvent atmosphere surrounding the measuring cell.

Acknowledgment. We thank Mr. M. Martineau and Ms. E. Sellier of the TEM facility CREMEM, Université Bordeaux 1. S.B. and this project have been supported financially by IFCPAR 3605-2. S.N.M. has received financial support by the CNRS. The authors thank the CNRS, the French Ministry of Education and Research, and the Région Aquitaine for financial support.

Supporting Information Available: Figures S1 and S2 (PDF). This material is available free of charge via the Internet at http://pubs.acs.org.